

ESD RECORD COPY

127

RETURN TO
SCIENTIFIC & TECHNICAL INFORMATION DIVISION
(ESTI), BUILDING 1211

COPY NR. _____ OF _____ COPIES

ESTIMATED PROPERTIES OF LAMINAR WAKES WITH COUPLED
RATE CHEMISTRY AND DIFFUSIONESTI PROCESSED DDC TAB PROJ OFFICER ACCESSION MASTER FILE _____

DATE

ESTI CONTROL NR.

AL-40802

by

CY NR. / OF / CYS

H. M. Bloom, R. W. Byrne and E. D. Kennedy

May 1962

Reissued September 18, 1962

The work reported in this document was performed at General Applied Science Laboratory, Inc. for M. I. T. Lincoln Laboratory under Subcontract No. 226; this work was supported by the U.S. Advanced Research Projects Agency under Air Force Contract AF 19(604)-7400 (ARPA Order 13).

When US Government drawings, specifications or other data are used for any purpose other than a definitely related government procurement operation, the government thereby incurs no responsibility nor any obligation whatsoever; and the fact that the government may have formulated, furnished, or in any way supplied the said drawings, specifications, or other data is not to be regarded by implication or otherwise as in any manner licensing the holder or any other person or conveying any rights or permission to manufacture, use, or sell any patented invention that may in any way be related thereto.

Qualified requesters may obtain copies from Defense Documentation Center (DDC). Orders will be expedited if placed through the librarian or other person designated to request documents from DDC.

Copies available at Office of Technical Services, Department of Commerce.

Do not return this copy. Retain or destroy.

Publication of this technical documentary report does not constitute Air Force approval of the report's findings or conclusions. It is published only for the exchange and stimulation of ideas.

ESTIMATED PROPERTIES
OF LAMINAR WAKES WITH
COUPLED RATE CHEMISTRY
AND DIFFUSION

TECHNICAL REPORT NO. 282

By H. M. Bloom, R. W. Byrne and E. D. Kennedy

SUBCONTRACT NO. 226

Prepared For

Massachusetts Institute of Technology
Lincoln Laboratory
Lexington 73, Massachusetts

Prepared By

General Applied Science Laboratories, Inc.
Merrick and Stewart Avenues
Westbury, L.I., New York

May, 1962

Approved by:

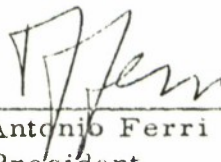

Antonio Ferri
President

TABLE OF CONTENTS

<u>Section</u>	<u>Title</u>	<u>Page</u>
	Abstract	1
I	Introduction	3
II	Distributions Along the Axis and "Lengths"	5
III	Sensitivity to Rate Constants	11
IV	Lewis and Prandtl Number Effects	13
V	Ratio of Diffusion to Chemical Production Terms	14
VI	Effect of Assuming and Augmented Magnitude of Viscosity	15
	References	16
	Tables I and II	17
	Notations	18
	Figures Nos. 1 to 12	19

ESTIMATED PROPERTIES OF LAMINAR WAKES WITH
COUPLED RATE CHEMISTRY AND DIFFUSION

M. H. Bloom, R. W. Byrne and E. D. Kennedy

ABSTRACT

Theoretical analyses bearing on wake observables required a careful representation of the rate chemistry of air and its coupling with diffusive processes. A selection of preliminary results of recent calculations of laminar, constant-pressure axisymmetric wakes, including chemical-diffusive coupling made for several full-scale flight and firing range conditions is presented. The analysis employs an integral method wherein the governing differential equations are satisfied exactly along the axis. The present chemical and thermodynamical models which consider N₂, N, O₂, O, NO, NO⁺ and e⁻ species are more detailed than those usually used in connection with wake calculations. However, the following assumptions are retained: a. vibrational equilibrium, b. Fick's law of diffusion for each species, c. a single representative Lewis number is taken constant and equal to 1.4, d. a constant value of the Prandtl number was taken as equal to 0.71.

Attention is devoted to the following items:

- a. Properties along the axis for representative reentry trajectories.
- b. Wake lengths associated with velocity, temperature, and density.
- c. Scaling considerations pertinent to a. and b.
- d. An indication of the sensitivity of the results to changes in the chemical rate constants.
- e. Sensitivity of the results to different assumed values of the Lewis and Prandtl numbers.
- f. The relative importance of diffusive and chemical terms evaluated along the axis in each equation of species concentration.
- g. The influence of a higher "effective" viscosity on the wake characteristics.

I INTRODUCTION

Theoretical analyses bearing on wake observables require a careful representation of the rate chemistry of air and its coupling with diffusive processes (see Refs. 1 and 2).

A preliminary selection of results of recent calculations of laminar, constant pressure, axisymmetric wakes including chemical-diffusive coupling, is presented here. The calculation is derived from an integral method analysis wherein the governing differential equations are satisfied exactly along the axis. The present chemical and thermodynamic models, which consider N_2 , N, O_2 , O, NO, NO^+ and e^- species, are more detailed than those previously described in connection with the wake calculations of Refs. 1 and 2 (the revisions are described in Ref. 3). However, the following assumptions are retained: (a) vibrational equilibrium, (b) Fick's law of diffusion for each species, (c) a single representative Lewis number taken constant and equal to 1.45, and (d) constant Prandtl number equal to 0.71. The calculations were made with an IBM 7090 digital computer. Conditions at the beginning of the far wake were obtained by means of an integration of the species rate equations, and the one-dimensional equations of energy and momentum along the body surface streamline from the stagnation point. The general method of calculation is described more fully in Ref. 4.

Results are presented of calculations about the Trailblazer II vehicle for the Lincoln Laboratory under the Reentry Physics Program.

Attention is devoted to the following items:

- a. Properties along the wake axis.
- b. Wake lengths associated with temperature and electron density, i.e., distances required for the indicated properties to decay to a specified level or degree of nonuniformity.
- c. Scaling considerations pertinent to (a) and (b).
- d. An indication of the sensitivity of the results to a number of changes in the rate constants (at one flight condition, assuming unchanged initial conditions).
- e. Sensitivity of the results to different assumed values of the Lewis and Prandtl numbers.
- f. The relative importance of diffusive and chemical terms evaluated along the axis in each equation of species concentration.
- g. The influence of a higher "effective viscosity" on the wake characteristics.

These items will be taken up in sequence.

II. DISTRIBUTIONS ALONG THE AXIS AND "LENGTHS"

Wake Lengths of properties dominated by diffusive processes are of order $\delta^2 \rho u / \mu$, where δ is a typical wake radius roughly proportional to $(C_D A)^{1/2}$ and $\rho u / \mu$ is evaluated at a significant reference condition, say a mean value of properties throughout the wake. For preliminary simplified discussion, the reference Reynolds number per foot $\rho u / \mu$ will here be evaluated in the free stream. Thus a scaling parameter for the axial coordinate or for wake lengths of diffusive processes is $\delta^2 \rho u / \mu$ or $C_D A (\rho u / \mu)$. For a given body, this scale factor depends only upon $\rho u / \mu$. Moreover, over much of a typical reentry trajectory, changes in ρ are more influential than changes in u / μ —hence diffusive lengths may be expected to scale roughly like ρ and increase monotonically during descent. The axial variation of temperature, velocity and electron density for Trailblazer II are shown in Figs. 1, 2 and 3 respectively. Figs. 4, 5, and 6 show the same parameters plotted in terms of a scaled length (the reference is the 200,000 ft. case) in accord with what has been said above. Complete correlation on this basis cannot be expected, particularly for properties of the flow which are significantly influenced by chemical rate processes. For example, the pronounced temperature peaks indicated in Fig. 1 are primarily the result of coupled diffusion and recombination of nitrogen atoms, the temperatures being particularly sensitive to small differences between the stagnation enthalpy and the sum of the kinetic energy per unit mass and the chemical

5

energy contribution to enthalpy. Furthermore, improved correlation is obtained when account is taken of the differences in initial conditions and of the influence of the elevated interior wake temperatures on the diffusion time $\delta^2 \rho / \mu$. For example, it has been shown analytically that in the present analysis u_0/u_e is primarily a function of the coordinate $(\rho_e u_e \theta_c / \mu) \int_{x_c}^x (\mu_0 / \mu_e) dx$, where $\theta_c = C_D A / 4\pi$. An approximate correlation of rate chemistry effects on the axial scale can be expected by a normalization of the axial coordinate with respect to $\mu u / \mu$ due to the fact that two-body collision processes take place roughly in proportion to ρ , whereas three-body collision processes, such as recombinations, take place in proportion to ρ^2 . The point here is that variations of u/μ during a trajectory are not as drastic as that of ρ and that at least a part of the ρ^2 scaling required for recombination will be provided by the ρ scaling. At low altitudes, where equilibrium chemistry prevails, the scaling applies to the velocity and enthalpy. The distribution of species then follows from the equilibrium conditions.

Examination of the plots of electron densities clearly shows that one must specify a species level before drawing a conclusion on the variation of an associated wake length. For example, at an electron density level of 10^9 , the wake lengths first increase during descent, then peak in the neighborhood of 140,000 feet in the present instance, and finally decrease as chemical equilibrium is approached. On the other hand, at very low levels like 10^7 or 10^6 electrons/cc, the wake length increases monotonically during descent.

The establishment of peak values of the concentrations is responsible for this type of phenomenon, and, as mentioned previously, the scaling considerations do not apply to the peak values.

The temperature and electron density plots also show equilibrium values (dashed lines). The equilibrium temperatures were obtained from a Mollier diagram for equilibrium air corresponding to the pressure and enthalpy determined in the nonequilibrium wake calculations. The equilibrium electron densities were calculated from the equilibrium of the reaction $N + O \rightleftharpoons NO^+ + e^-$ at the density, temperature, and atom mass fractions of the nonequilibrium calculation. As would be expected on the basis of the nonequilibrium calculations employed to determine the initial conditions of the wake, the equilibrium temperatures are much higher than the nonequilibrium values at first. Further downstream, the nonequilibrium temperatures, substantially affected by chemical processes at low altitudes, diffusion at high altitudes, and coupled effects in between, drive toward equilibrium and indeed may overshoot the equilibrium values. This produces the peak temperatures shown in the nonequilibrium cases. The decrease in the initial slope of the temperature curve during descent shows the decreasing relative influence of diffusion with decreasing altitude. At the lowest altitude (100,000 ft.), this effect and the very much reduced flight speed combine to yield the monotonic trend toward equilibrium. Downstream of the region of peak temperatures, the nonequilibrium temperatures approach the equilibrium

values, although differences on the order of 20% or more may still be in evidence before the very far wake is reached. In the very far wake, the non-equilibrium temperatures of course approach the equilibrium values.

Consider now the electron densities. In this discussion, the term "equilibrium" in regard to electrons refers to the $N + O \rightleftharpoons NO^+ + e^-$ reaction in the nonequilibrium bath provided by the other species. It is seen that at the intermediate altitudes, the nonequilibrium electron densities, which are initially higher than the equilibrium values, drive strongly down toward equilibrium and then follow the equilibrium values closely, peaking along with them. At these altitudes, the distributions are clearly insensitive to the initial values. At the lowest altitude (100,000 ft), there is the same drive down to equilibrium. However, in this case, the equilibrium values exhibit no peak, or at most a weak spread-out peak, due to the lower energy of the flight condition. Hence the nonequilibrium electron density exhibits no peak.

At the high altitudes, the equilibrium distributions do peak, but the nonequilibrium values which are strongly influenced by diffusion and drive down toward the equilibrium values, may or may not intersect the equilibrium peaks. The reason for this is that the nonequilibrium temperatures to which the "equilibrium" electron densities correspond, are simply not high enough to produce peak equilibrium electron densities of sufficient magnitude to meet the initially-high nonequilibrium values. As a result of this (as well as

strong diffusion) peaks in nonequilibrium electron densities are either small or nonexistent at high altitudes.

Another indication of the possibility of scaling the wake results is given in the comparison between the full-scale Trailblazer II wake results calculated for the 150,000-foot altitude case with the wake results obtained for a pellet of the same geometry but reduced in size by a factor of 24.5 and fired in a range at approximately the same ambient conditions. The pellet firing range conditions for which the wake was calculated correspond to a velocity of 22, 100 fps and a pressure of 1 mm Hg. These correspond closely to the full-scale conditions for the 150,000-foot altitude case for the full-scale Trailblazer II (Table I). A comparison of electron densities along the wake axis is shown in Fig. 7. Major diffusion effects are extracted by use of the coordinate scale $(D_1/D_2)^{1/2}x$ for the small pellet. Since nonequilibrium effects over the body have been taken into account in establishing the initial conditions in both cases, the initial values shown in Fig. 7 differ by an order of magnitude, the more frozen pellet values being higher than those of the larger body. To remove some effect of the difference in initial conditions, the pellet values are also shown divided by 10 (dashed curve). The short diffusion times in the pellet wake prevent the formation of a peak in electron density, despite the fact that significant temperature rises are produced simultaneously due to diffusion of the major atomic species. The influence of chemical effects is also exhibited by the fact that the electron densities of the large body are lower than those of the pellet. This is so

beyond the peak region even when the influence of the initial values is normalized out (dashed curve). This trend is consistent with that shown in Fig. 3 which shows equilibrium electron densities (at the nonequilibrium state) lower than those given by the nonequilibrium electron-producing reaction.

III. SENSITIVITY TO RATE CONSTANTS

Within the framework of detailed calculations of wake chemistry it is of interest to inspect the influence of changes in values of the rate constants, since the values used originally and incorporated in the IBM 7090 program were those suggested in Ref. 5 as being within the current state of the art. They are admittedly crude estimates in some cases and are subject to further revision. Newly suggested values (Ref. 6) differ from the former values in the temperature range of interest, in some instances by factors on the order of 5. In the present calculations a number of changes in the rate constants were made using the important 150 Kft flight condition for the Trailblazer II trajectory.

Reaction rates for the following three reactions were varied by factors of 10 and 10^{-1} from the original values found in Reference 5.



The corresponding reaction rates from Ref. 5 and used in Ref. 3 are

$$Kr_a = .5 \times 10^5 \times (T/4500)^{-1.5}, \text{ cm}^6/\text{mole}^2\text{sec}$$

$$Kr_b = 3 \times 10^{-3} \times T^{-3/2}, \text{ cm}^3/\text{sec/part}$$

$$Kr_c = 2/3 \times 10^{14} \times (T/4500)^{-1.5}, \text{ cm}^6/\text{mole}^2\text{sec}$$

The rates Kr_a , Kr_b , Kr_c were varied one at a time to give the results shown in Figure 8, where the axis electron density values in the wake are

given for each of the cases shown in Table II.

It is emphasized that the initial conditions which would also be subject to change due to changes in reaction rates were kept the same for the present test. It is seen that the changes in electron densities in general are not drastic. The only significant change in the results is brought about by slowing down the electron-producing reaction by a factor of 10^{-1} (Case 5). Increases in the rate constants are less influential than this decrease in the electron-forming rate constant.

IV. LEWIS AND PRANDTL NUMBER EFFECTS

Indications of the importance of the values of the Lewis and Prandtl numbers on the diffusion of species and on the temperatures have been given in References 1 and 2. The sensitivity of the temperatures to these factors is due primarily to the small enthalpy differences cited previously, which are affected significantly by species concentrations through their effect on the reaction energy.

Wake calculations were made for three sets of values of Lewis and Prandtl number for the 150,000 ft altitude case on the Trailblazer II trajectory. The values of the Lewis and Prandtl number used throughout the calculations discussed above were 1.45 and .71 respectively. The two additional pairs of values for which the wakes were calculated are ($Le = 1.0$, $Pr = 0.71$) and ($Le = 1.0$, $Pr = 1.0$).

The results of these calculations, plotted in Figure 9 show that the temperature peak is lowest when the Prandtl and Lewis numbers are unity. The peak is raised when the Prandtl number is 0.71 and the Lewis number is unity. The highest temperatures are obtained when the Prandtl number is 0.71 and the Lewis number 1.4. The corresponding electron densities given in Figure 10 exhibit the same trend.

V. RATIO OF DIFFUSION TO CHEMICAL PRODUCTION TERMS

To assist in understanding the indicated trends more deeply the ratio of the diffusion to the chemical-rate term in each species-conservation differential equation was calculated. These are shown in Figure 11 for the representative Trailblazer II, 150 Kft case for the initial portion of the wake. In this figure the dashed line indicates that the diffusive term is negative for the given species, hence the sign of the chemical term can be deduced from the figure.

An interesting result is that the chemical effect on the electron-producing reaction is dominant at the start of the wake and probably diminishes in importance downstream. It is reasonable to expect that diffusion will dominate the wake behavior over the large downstream extent.

More detailed studies of the type indicated are in preparation.

I. EFFECT OF ASSUMING AN AUGMENTED MAGNITUDE OF VISCOSITY

In studies of the effect of turbulence on mean properties, many arbitrary assumptions must be made, particularly with regard to turbulent transports in flows with thermal and chemical effects. In this spirit and because a calculation would be made conveniently, it was decided to simulate very crudely the influence of turbulence in the coupled diffusive-chemical-rate calculation by simply altering the magnitude of the laminar molecular viscosity coefficient. The diffusive and thermal transports were in effect augmented in the same proportion since the Prandtl and Lewis numbers were kept the same as the laminar values. Thus an "effective viscosity" independent of velocity gradient was introduced. A set of results for electron-density distributions according to this rough model is shown in Figure 12, where the laminar μ is multiplied by factors of 10 and 100.

The effect of this assumption is to decrease the diffusion time and Reynolds number while the reaction times and particle residence times are unchanged. This would not be the case if factors like density, velocity or body size were altered. The results show the sharply reduced electron levels. This reduction is caused not only by simple diffusion, but also by the coupled reactions as is demonstrated by the scaled representations shown dashed. The scales of the dashed curves are indicated multiples of the physical scale, and would correlate a purely diffusive phenomenon.

REFERENCES

1. Bloom, M. H. and Steiger, M. H., Hypersonic Axisymmetric Wakes Including Effects of Rate Chemistry, General Applied Science Laboratories, Inc., Technical Report 180, August 1960.
2. Vaglio-Laurin, R. and Bloom, M. H., Chemical Effects in External Hypersonic Flows, International Hypersonics Conference Paper 1975-61, Mass. Institute of Technology, August 1961.
3. Steiger, M. H., Improved Hypersonic Laminar Wake Calculations Including Rate Chemistry, General Applied Science Laboratories, Inc. Technical Report 249, August 1961.
4. Kennedy, E., Fields, A., and Seidman, M., The Calculation of the Flow Field about a Blunted 9° Cone, Section I - Characteristics Calculations, General Applied Science Labs., Inc. Technical Report 256, November 1961
5. Wray, K., Teare, J. D., Kivel, B., and Hammerling, P., Relaxation Processes and Reaction Rates Behind Shock Fronts in Air and Component Gases, Avco-Everett Research Laboratory, Research Rpt. 83, December 1959.
6. Wray, Kurt L., Chemical Kinetics of High Temperature Air, International Hypersonics Conference Paper 1975-61, Massachusetts Institute of Technology, August 1961.

TABLE I
FLIGHT CONDITIONS

Trailblazer II

<u>Altitude</u> <u>(thousands of ft)</u>	<u>Velocity</u> <u>(fps)</u>
100	15,875
150	21,600
200	22,475
250	22,550

TABLE II
VARIATIONS OF REACTION RATES USED

1. no change
2. $Kr_a \times 10$
3. $Kr_a \times 10^{-1}$
4. $Kr_b \times 10$
5. $Kr_b \times 10^{-1}$
6. $Kr_c \times 10$
7. $Kr_c \times 10^{-1}$

NOTATIONS

A reference area for drag

D Drag

C_D body drag coefficient (D/A) $\left/ \left(\mu_e u_e^2 / 2 \right) \right.$

n_e electron density, electrons/cc

u streamwise velocity

x streamwise coordinate (ft)

δ wake radius

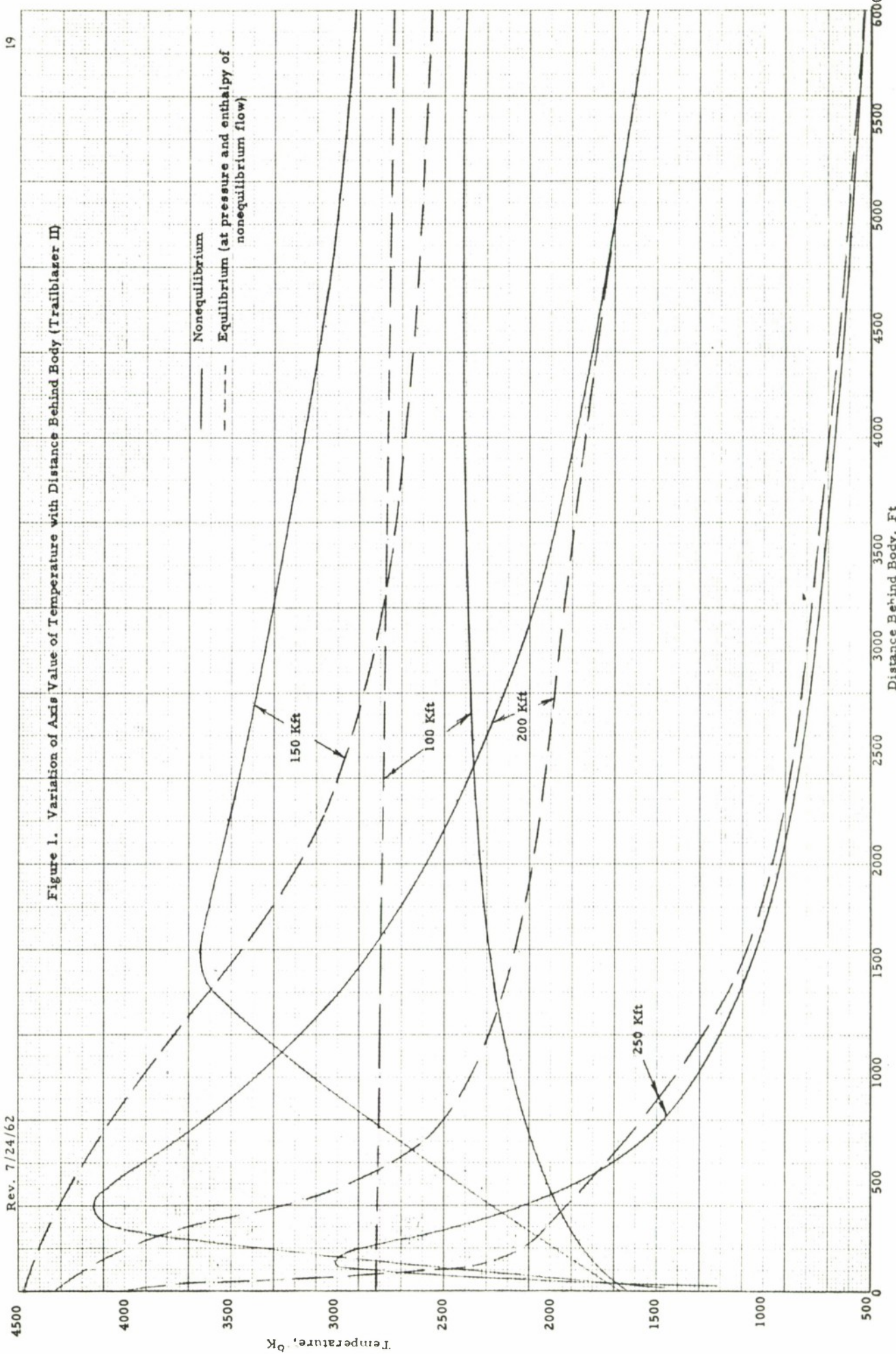
ρ density

μ absolute viscosity

Subscript

c free-stream (undisturbed) conditions

o axis conditions



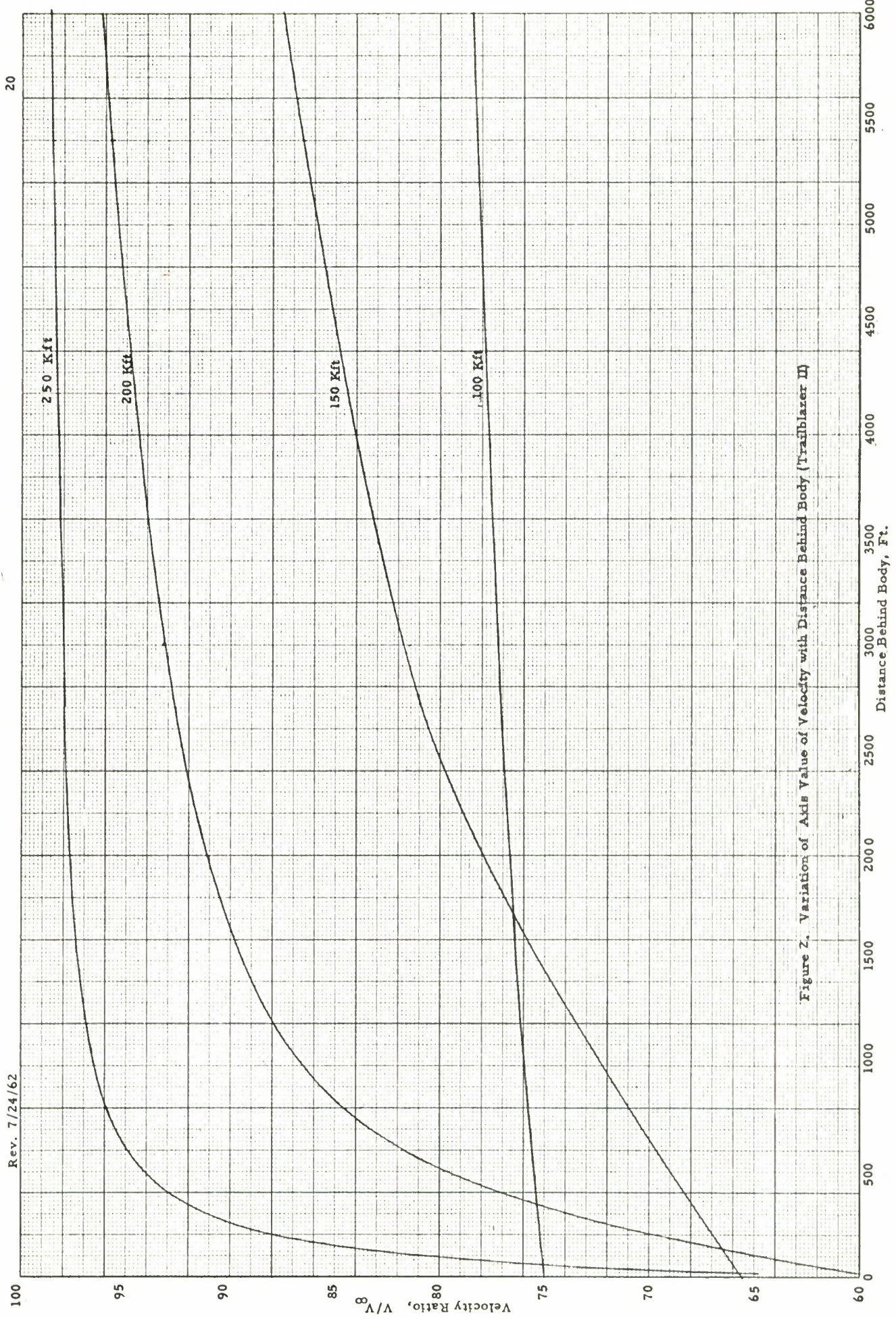


Figure Z. Variation of Axis Value of Velocity with Distance Behind Body (Trailblazer II)

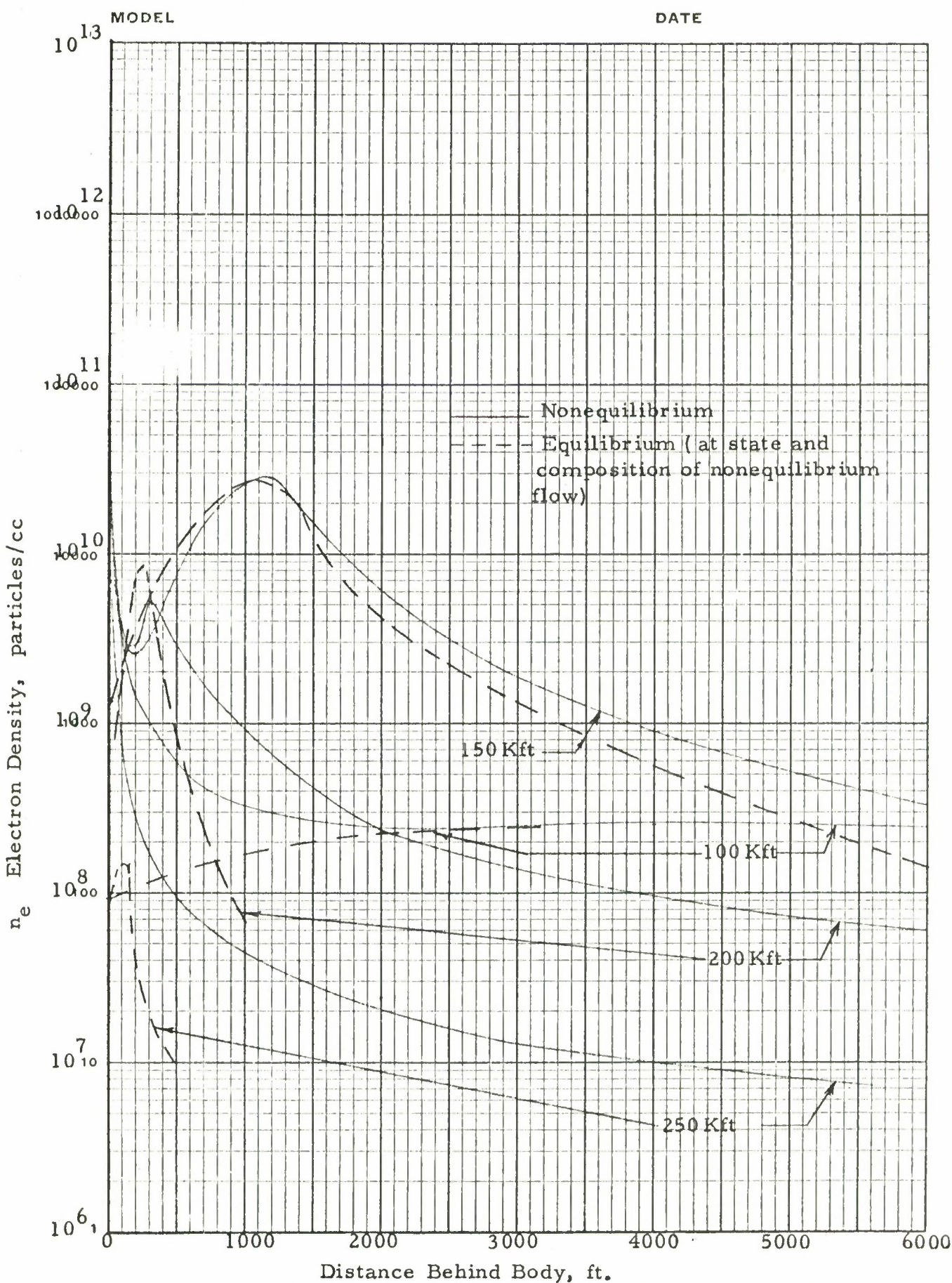
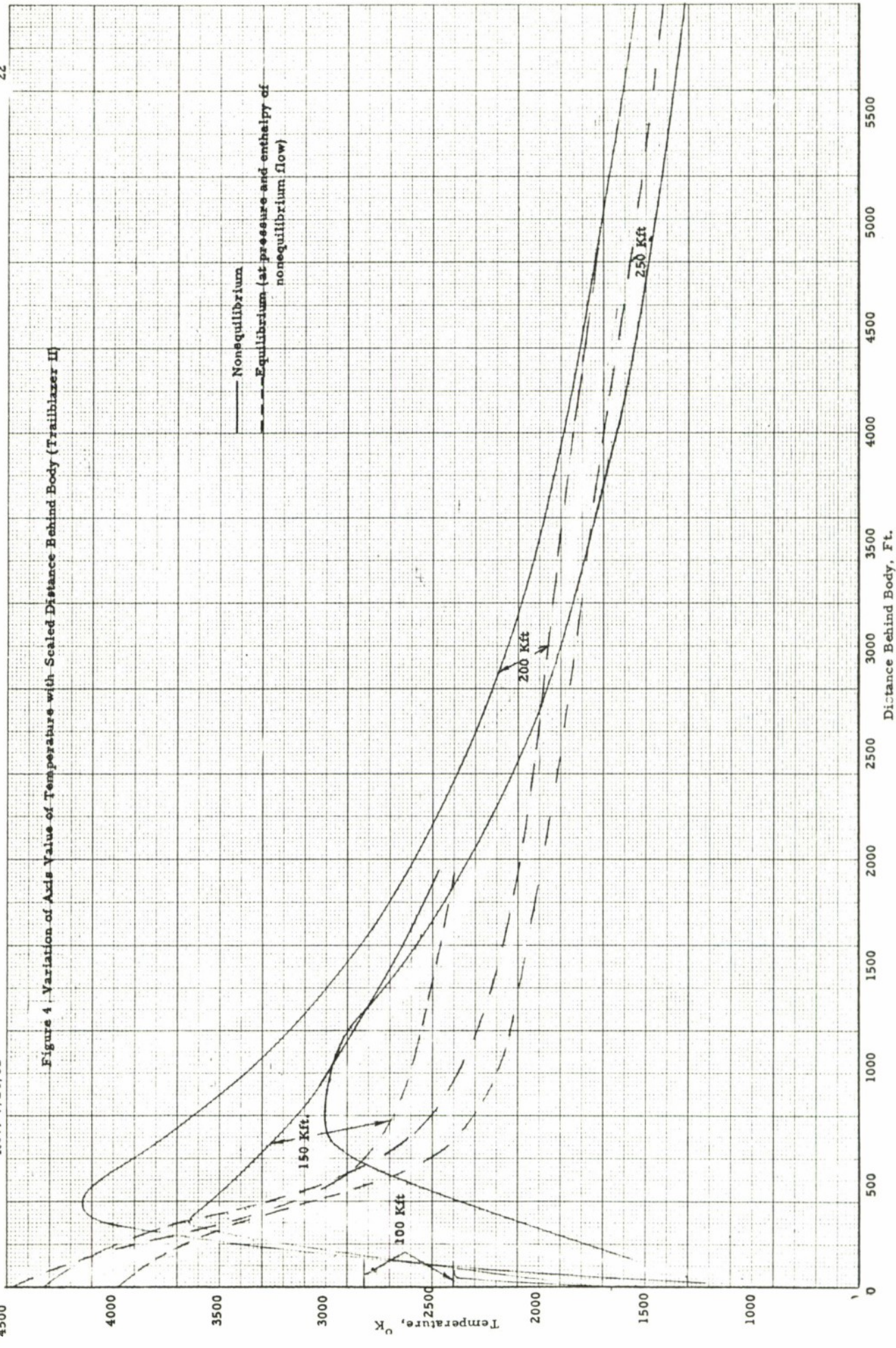


Figure 3 . Variation of Axis Value of Electron Density with Distance Behind Body (Trailblazer II)

Figure 4. Variation of Axis Value of Temperature with Scaled Distance Behind Body (Trailblazer II)



Rev. 7/24/62

23

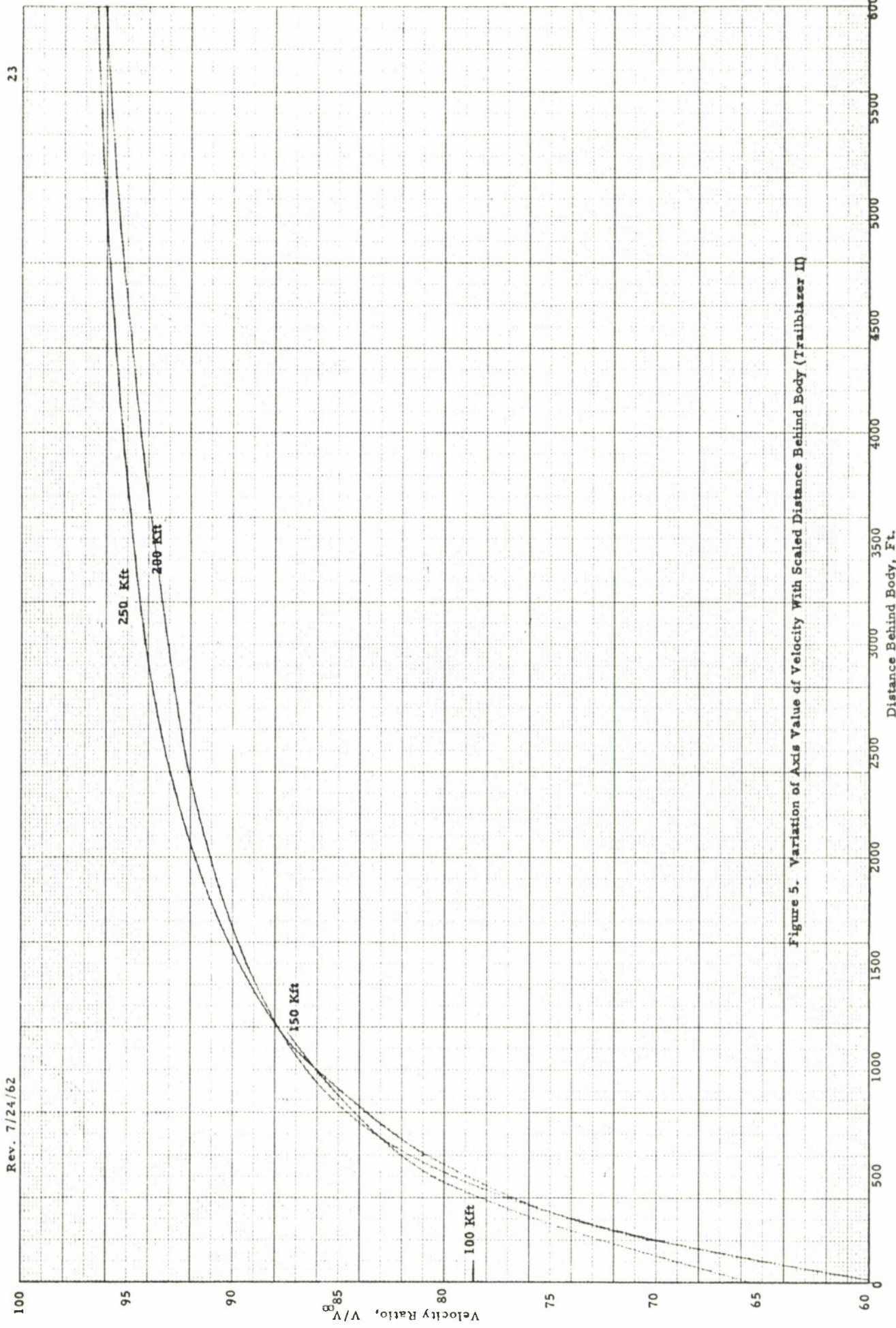
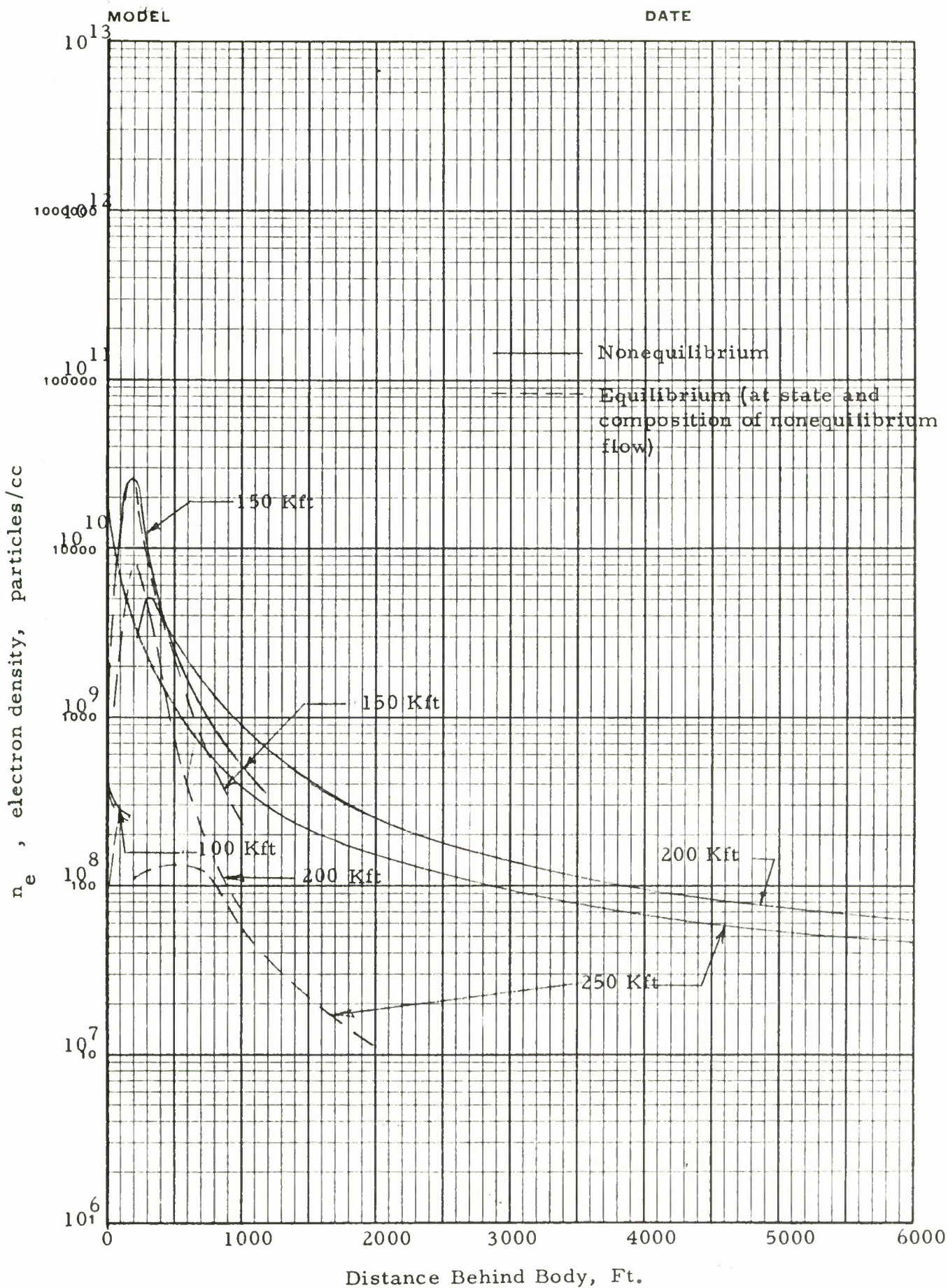


Figure 5. Variation of Axis Value of Velocity With Scaled Distance Behind Body (Trailblazer II)

Figure 6 Variation of Axis Value of Electron Density with Scaled Distance Behind Body



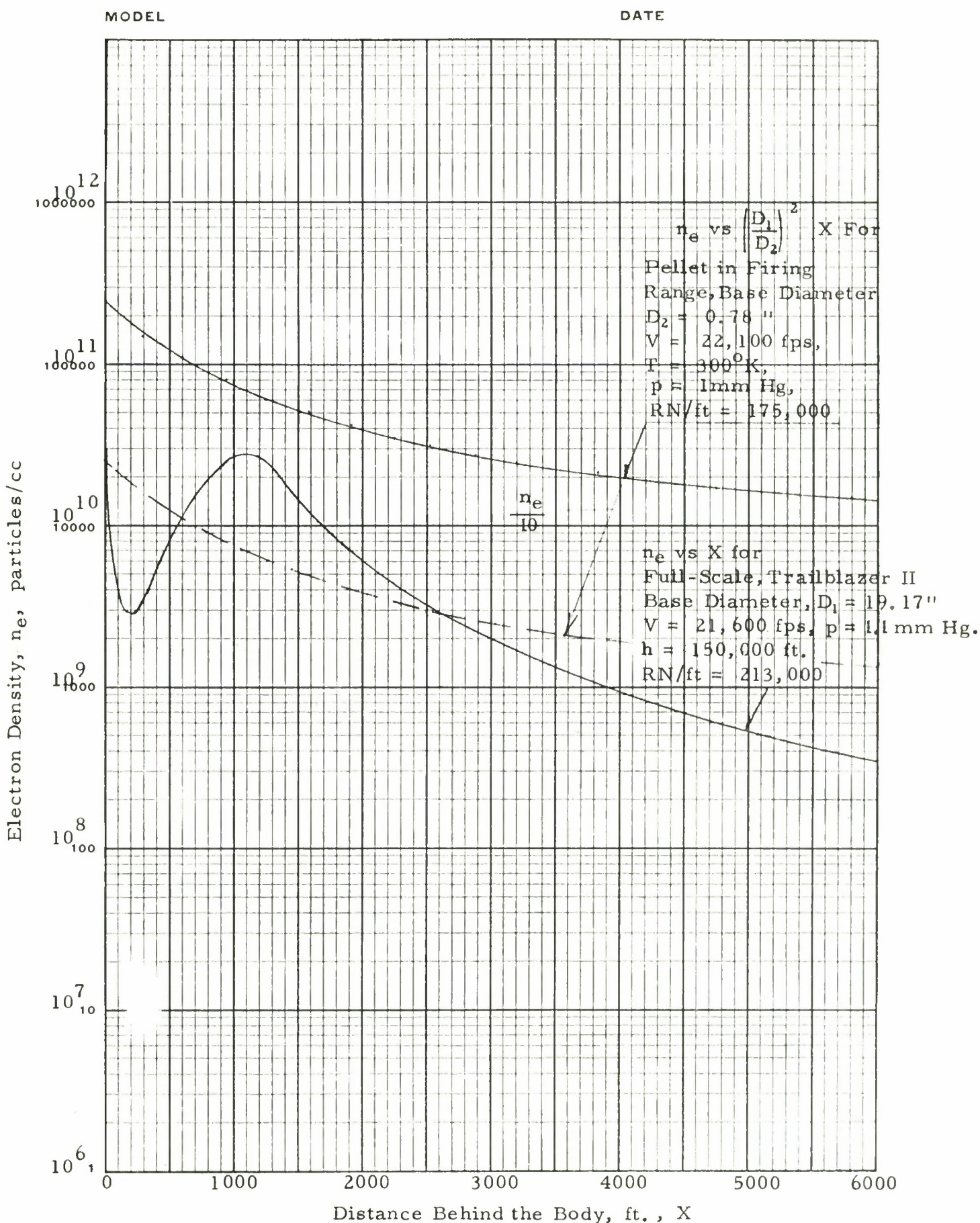
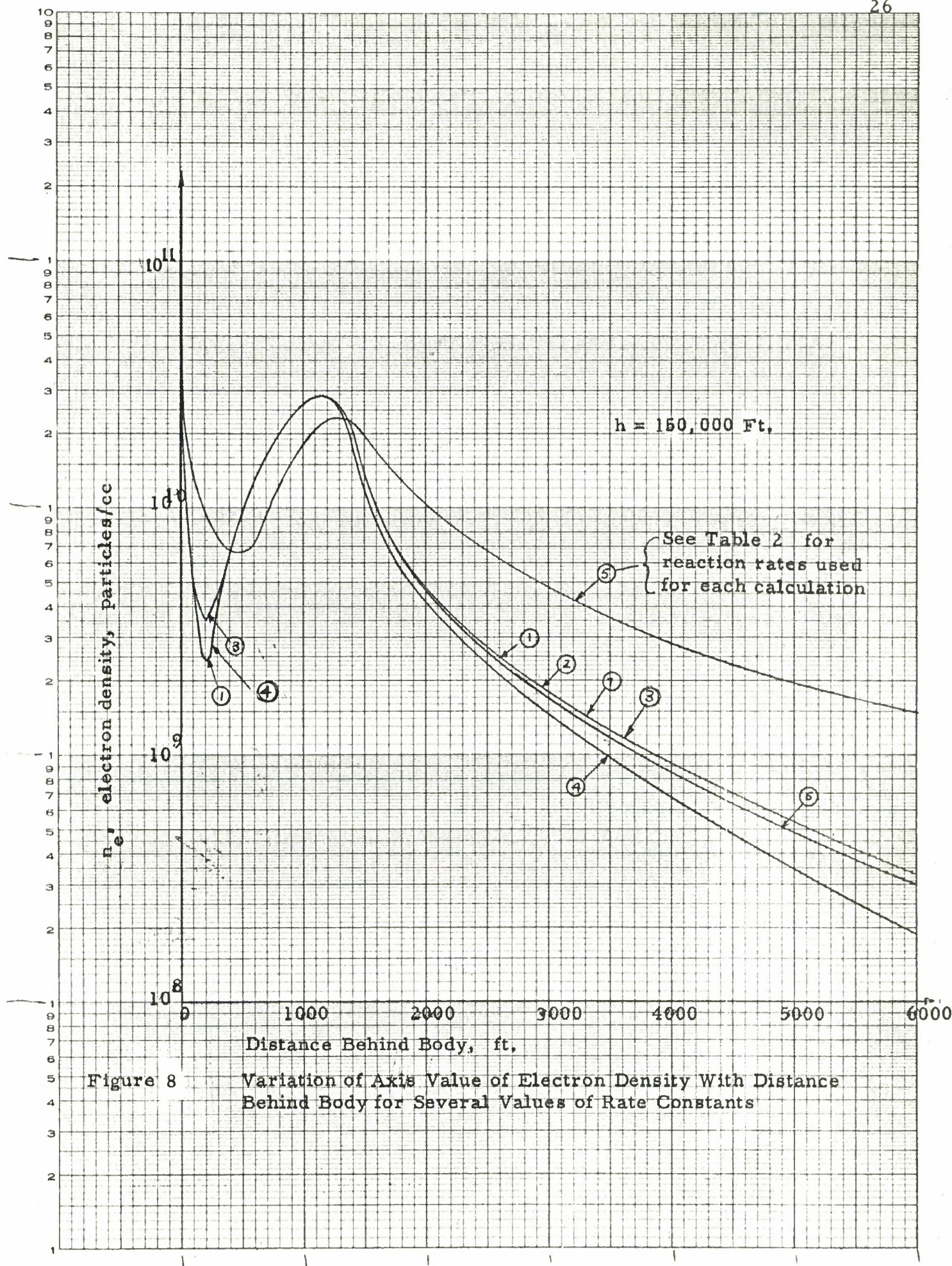
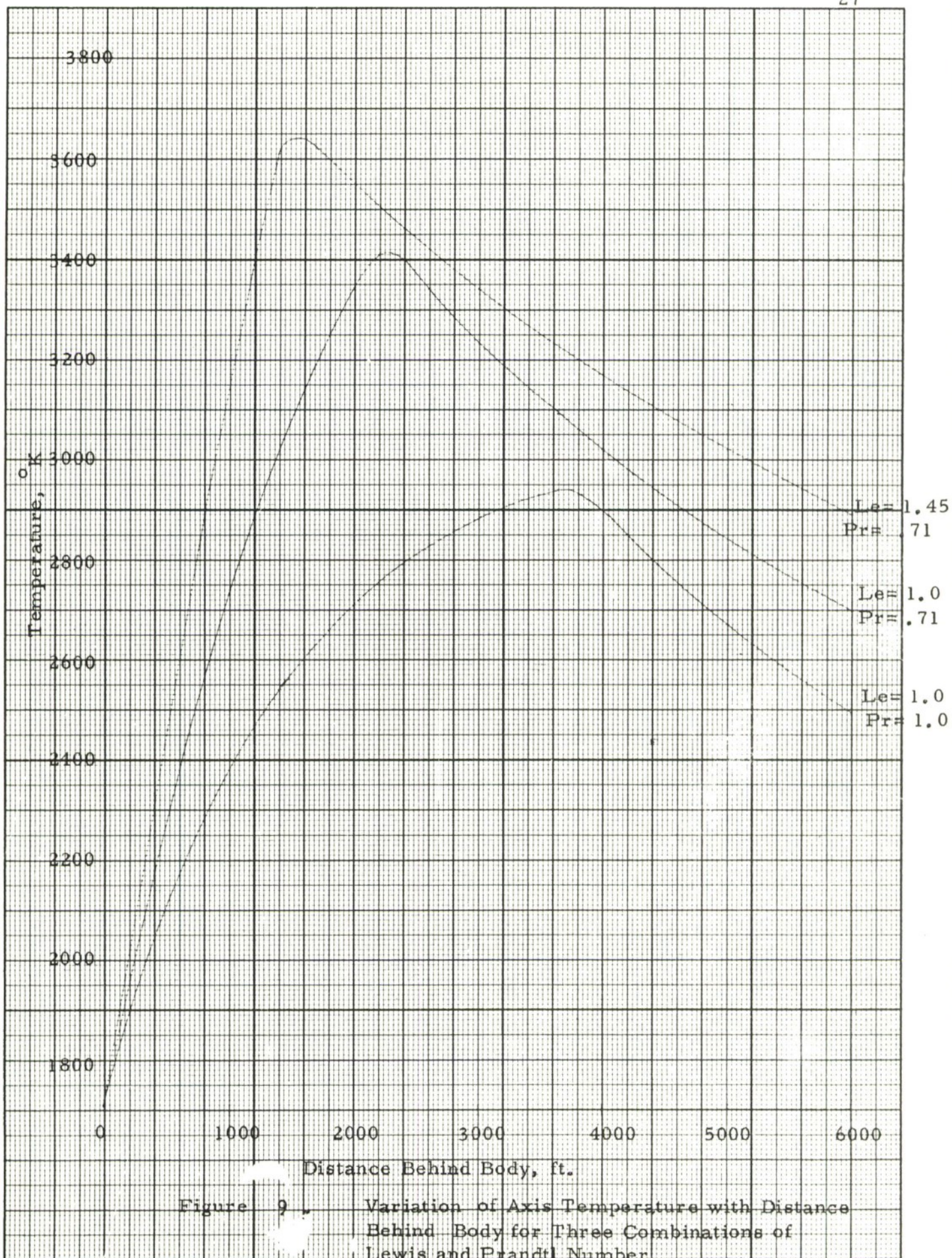
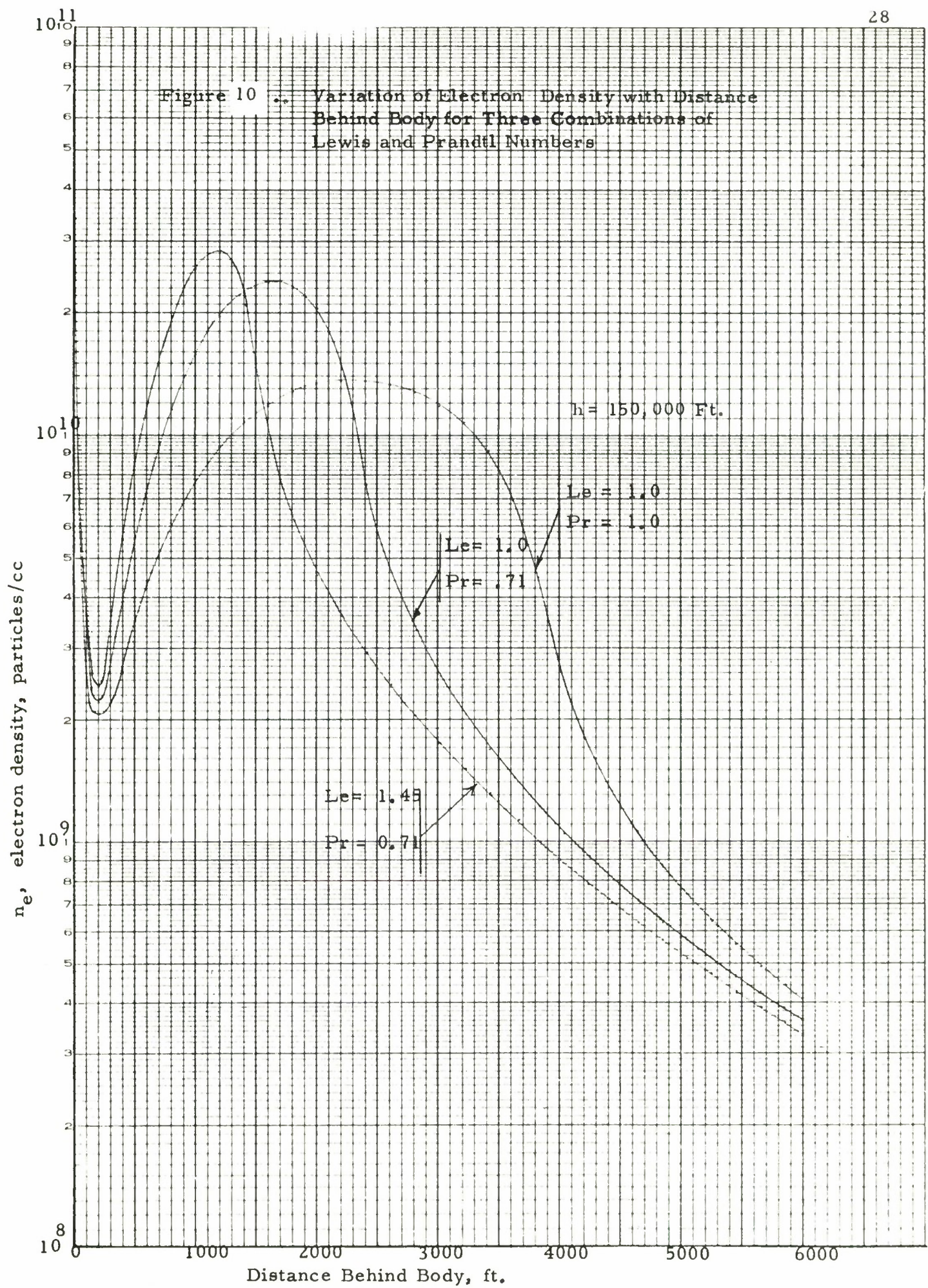


Figure 7 • Comparison of Calculated Wakes for Pellet and Full-Scale Vehicle. Axis Values of Electron Density Versus Distance Behind the Body







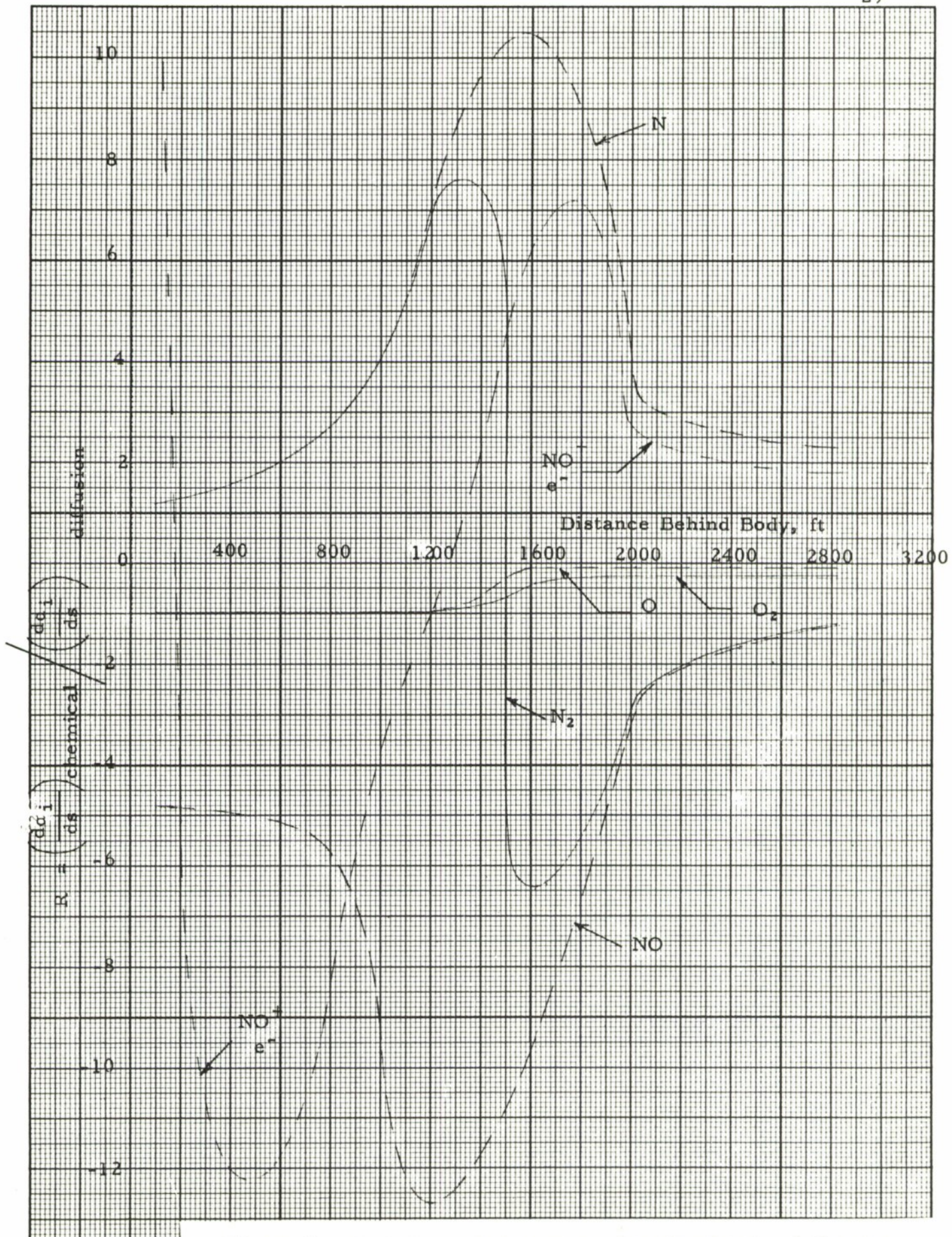


Figure 11. Variation with Distance of Ratio of Rate of Change of Specie Mass Fraction Due to Chemical Production to that Due to Diffusion.

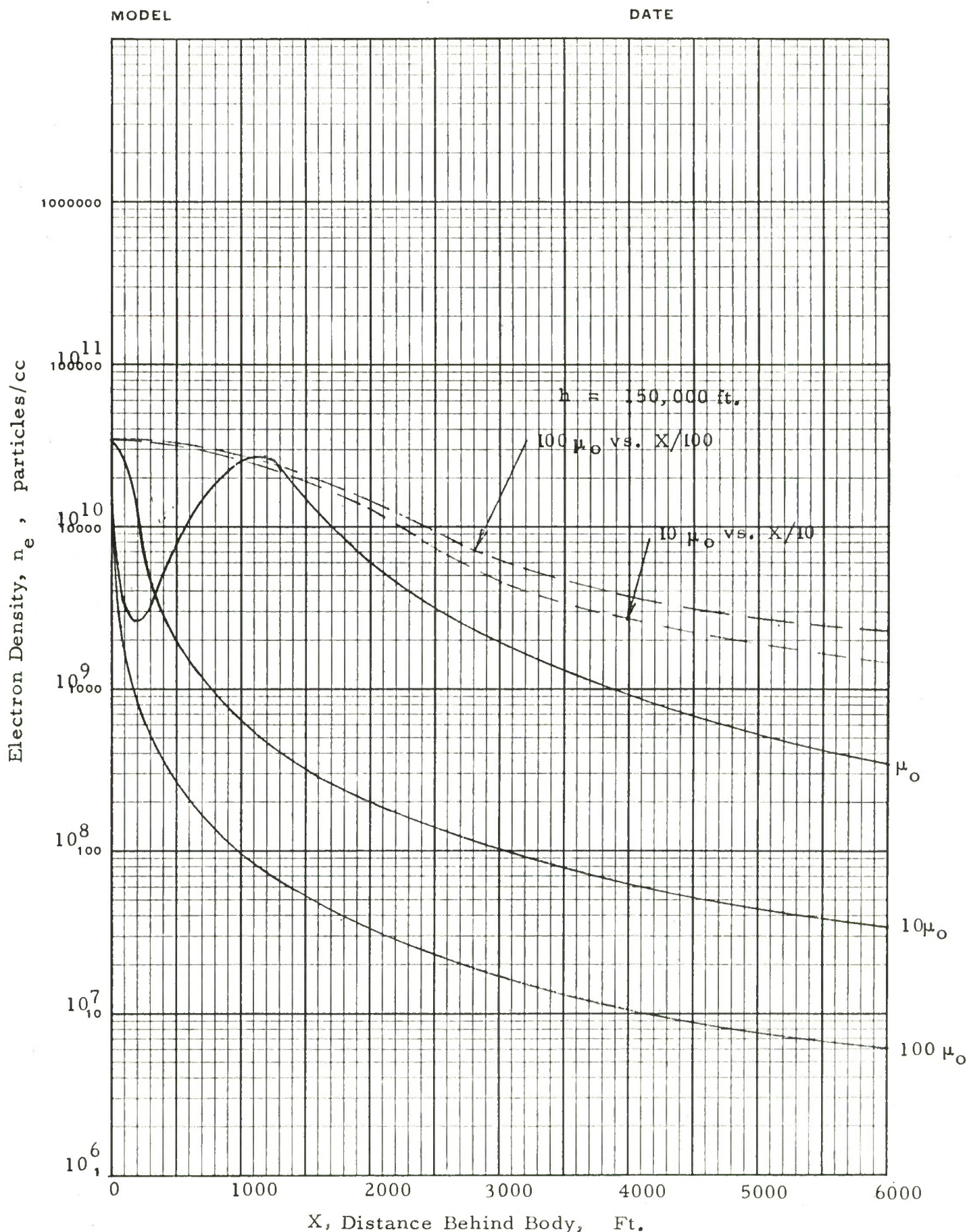


Fig. 12 . The Effect of Viscosity on the Distribution of Electron Density on the Wake Axis.